

**Converging sequences in the *ab initio* no-core shell model**

C. Forssén\*

*Department of Fundamental Physics, Chalmers University of Technology, SE-412 96 Göteborg, Sweden*

J. P. Vary

*Department of Physics and Astronomy, Iowa State University, Ames, Iowa 50011, USA*

E. Caurier

*Institut de Recherches Subatomiques (IN2P3-CNRS-Université Louis Pasteur) Batiment 2711, F-67037 Strasbourg Cedex 2, France*

P. Navrátil

*Lawrence Livermore National Laboratory, P. O. Box 808, L-414, Livermore, California 94551, USA*

(Received 18 September 2007; published 4 February 2008)

We demonstrate the existence of multiple converging sequences in the *ab initio* no-core shell model. By examining the underlying theory of effective operators, we expose the physical foundations for the alternative pathways to convergence. This leads us to propose a revised strategy for evaluating effective interactions for  $A$ -body calculations in restricted model spaces. We suggest that this strategy is particularly useful for applications to nuclear processes in which states of both parities are used simultaneously, such as for transition rates. We demonstrate the utility of our strategy with large-scale calculations in light nuclei.

DOI: [10.1103/PhysRevC.77.024301](https://doi.org/10.1103/PhysRevC.77.024301)

PACS number(s): 21.60.Cs, 03.67.Lx, 21.30.Fe, 27.20.+n

**I. INTRODUCTION**

The *ab initio* no-core shell model (NCSM) is a method to solve the full  $A$ -body problem for a system of nonrelativistic particles that interact by realistic two- plus three-body forces. A particular feature of the method is the use of effective interactions appropriate for the large, but finite, harmonic-oscillator (HO) model spaces employed in the calculations. Over the last few years, the NCSM method has been established as a very valuable tool in nuclear physics, aiming for an exact description of nuclear structure starting from the fundamental interaction between nucleons [1–3].

The objective of this paper is to highlight the existence of multiple converging sequences in the NCSM, and the opportunities that this property provides in practical applications. In particular, we will discuss and illustrate a specific converging sequence that relies on the implicit freedom in the choice of model-space cutoff when constructing the cluster-approximated effective interactions used in the NCSM. These effective interactions are intended to take into account effects of configurations outside the model space. In general, the effective interaction is derived from the underlying realistic internucleon potential by a unitary transformation [4–8]. The procedure aims to reproduce exactly a subset of the eigenvalues to the original Hamiltonian in the finite model space. The effective interaction, in principle, becomes an  $A$ -body operator but is, in practice, usually approximated at the  $a$ -body operator level, where  $a < A$ . This cluster approximation generates, e.g., a dependence on the choice of HO frequency,  $\hbar\Omega$ . However, the construction guarantees convergence to the exact solution, for any value of  $\hbar\Omega$ , as the size of the model space increases.

This guarantee holds independent of the relationship between the model space used to evaluate the cluster approximation and the model space used to carry out the diagonalization of the resulting  $A$ -body operator, as long as both increase. In addition, we note that for any finite model space of dimensionality  $d_P$ , and in the limit  $a \rightarrow A$ , we obtain exact solutions for  $d_P$  states of the full problem, with flexibility for the choice of physical states subject to certain conditions [9]. Thus, there is an arbitrary number of sequences in the NCSM that all converge, in principle, to the same result.

The implicit freedom in generating approximated effective interactions, as mentioned above, will be introduced in Sec. II in connection to a brief description of the NCSM formalism. The strategy that we propose to employ for certain applications has several advantageous properties compared to the traditional strategy for evaluating effective interactions. These properties will be discussed in Sec. III, while the features and applicability of the revised strategy will be illustrated in Sec. IV. The ideas presented in this paper are substantiated by large-scale calculations for light nuclear systems. However, we note that our revised strategy was already utilized in two recent papers applying the NCSM to heavier systems (with  $A = 47$ – $49$ ) in restricted many-body model spaces [10,11]. Conclusions and perspectives are presented in Sec. V.

**II. THEORY**

The goal is to solve the  $A$ -body Schrödinger equation with an intrinsic Hamiltonian  $H_A = T_{\text{rel}} + \mathcal{V}$ , where  $T_{\text{rel}}$  is the relative kinetic energy and  $\mathcal{V}$  is the sum of two-body nuclear and Coulomb interactions. The NCSM method also allows for the inclusion of three-body forces [12]. However, while realistic three-nucleon forces have been shown to

\*c.forssen@fy.chalmers.se

be important in obtaining the nuclear spectra [12–14] and in describing electromagnetic and weak form factors [15], we consider only two-body interactions in this study. We solve the many-body problem in a finite HO basis space and the usual approach is therefore to derive a model-space dependent effective Hamiltonian. For this purpose, we perform a unitary transformation of the Hamiltonian, in the spirit of Da Providencia and Shakin [4] and Lee, Suzuki, and Okamoto [5–8], which is able to accommodate short-range correlations. However, the very first step is to add a center-of-mass (c.m.) HO Hamiltonian to the intrinsic Hamiltonian. In the full Hilbert space the added  $H_{\text{c.m.}}^{\Omega}$  term has no influence on the intrinsic properties. When we introduce our cluster approximation below, the added  $H_{\text{c.m.}}^{\Omega}$  term generates a real dependence on the choice of HO frequency, but it also facilitates faster convergence to exact results with increasing basis size.

Note that even if the original Hamiltonian contained just one- and two-body terms, the transformed Hamiltonian  $\mathcal{H}$  contain up to  $A$ -body terms. Obtaining the exact transformation operator is equivalent to solving the initial problem, which would make the procedure impractical. Therefore, we introduce the cluster approximation. The approximation consists in obtaining the effective interaction from the decoupling condition between the model space ( $P$ ) and the excluded space ( $Q$ ) for the  $a$ -body problem, where  $a \leq A$ , and then using the effective interaction thus obtained in the desired  $A$ -body problem. See, e.g., Refs. [1,2,16] for details on the procedure. This approximation introduces a real dependence on the oscillator parameter  $\hbar\Omega$ . The resulting effective  $a$ -body effective interactions also depends on the nucleon number  $A$  and on  $N_{\text{max}}$ , the maximum  $A$ -body HO excitation energy defining the model space. The usual approach to handle the  $\hbar\Omega$ -dependence is to search for a range of  $\hbar\Omega$  values over which the results are weakly  $\hbar\Omega$ -dependent. This empirical choice then corresponds to the optimal HO frequency for the system.

There are two limiting cases of the cluster approximation: First, when  $a \rightarrow A$ , the solution becomes exact; a higher-order cluster is a better approximation and was shown to increase the rate of convergence [13]. Second, when  $P \rightarrow 1$ , the effective interaction approaches the bare interaction; and as a result, the effects of the cluster approximation can be minimized by increasing as much as possible the size of the model space.

In this work, we present results obtained at the two-body cluster level. In practice, the exact (to numerical precision) solutions for the  $a = 2$  cluster are obtained in basis spaces of several hundred  $\hbar\Omega$  in each relative motion  $NN$  channel. The resulting effective Hamiltonian, now consisting of a relative two-body operator, and the subtracted pure  $H_{\text{c.m.}}^{\Omega}$  term introduced earlier, is then inserted into an  $m$ -scheme Lanczos diagonalization process to obtain the  $A$ -body,  $P$ -space eigenvalues and eigenvectors. The evaluation of the  $A$ -nucleon Hamiltonian and its diagonalization is a highly nontrivial problem due to the very large dimensions we encounter. For the present work, we performed the many-body calculation with two completely independent shell-model codes: a specialized version of the code ANTOINE [17]; and the many-fermion dynamics MFD shell-model code [18]. At the diagonalization stage we also add the Lawson projection term,  $\beta(H_{\text{c.m.}}^{\Omega} - \frac{3}{2}\hbar\Omega)$

(with  $\beta$  being a large positive coefficient) to separate the physically interesting states with  $0s$  c.m. motion from those with excited c.m. motion. We retain only the eigenstates with pure  $0s$  c.m. motion when evaluating observables. All observables that are expressible as functions of relative coordinates, such as the rms radius and radial densities, are then evaluated free of c.m. motion effects.

### III. CONVERGING SEQUENCES

We define our  $P$ -space to consist of all  $A$ -body configurations in the oscillator basis with total oscillator energy less than or equal some cutoff value  $(N_m + 3A/2)\hbar\Omega$ , where  $N_m = N_{\text{min}} + N_{\text{max}}$ , and  $N_m$  is the sum of  $2n + l$  values of the occupied single-particle states in the configuration.  $N_{\text{min}}$  is the minimum value required by the Pauli principle. As an example,  $N_{\text{min}} = 2$  for  ${}^6\text{Li}$ . The  $P$ -space is equally described by the cutoff parameter  $N_{\text{max}}$ , that begins with 0. We note that the usual convention is to solve only for states whose parity corresponds to the configurations in the maximum subspace governed by  $N_{\text{max}}$ . The opposite-parity states are then obtained in the  $N_{\text{max}} + 1$  model space. The corresponding two-body cluster model space,  $P_2$ , is defined by the range of two-body states encountered in the  $P$ -space. This implies that the relative  $(n, l)$  states are restricted by the condition  $2n + l \leq N_m - N_{\text{spsmin}}$ , where  $N_{\text{spsmin}}$  denotes the minimum possible number of HO excitations of the  $(A - 2)$  spectators. Consider, e.g., a  ${}^6\text{Li}$  calculation in the  $N_{\text{max}} = 4$  model space. In this case  $N_m = 6$  and  $N_{\text{spsmin}} = 0$  (since the 4 spectator nucleons can all fit in the  $0s$  shell), which leads to a two-body cutoff at  $2n + l \leq 6$ .

Due to our cluster approximation a dependence of our results on  $N_{\text{max}}$  and on  $\hbar\Omega$  arises. For a fixed cluster size  $a$ , the smaller the basis space, the larger the dependence on  $\hbar\Omega$ . The residual  $N_{\text{max}}$  and  $\hbar\Omega$  dependences can be used to infer the uncertainty in our results arising from the neglect of effective many-body interactions.

The usual NCSM strategy has been to evaluate  $H_{\text{eff}}$  for each  $A$ -body model space. This strategy leads to the use of separate  $H_{\text{eff}}$  for positive- and negative-parity states. The convergence of, e.g., the energy spectrum of natural-parity states is then observed by performing calculations in a sequence of model spaces  $N_{\text{max}} = 0, 2, 4, \dots$ , with corresponding effective interactions, while unnatural-parity states are obtained in the  $N_{\text{max}} = 1, 3, 5, \dots$  sequence. However, the theory guarantees convergence to the exact results of any sequence that follows a simple rule and brings us to the full  $A$ -body Hilbert space ( $P \rightarrow 1$ ) as the model space is increased. In particular, we can consider the following rule for evaluating the effective Hamiltonian:

$$N_{\text{max,eff}} = N_{\text{max}} + N_{\text{shift}}, \quad (1)$$

where convergence is obtained for  $N_{\text{max}} \rightarrow \infty$ , and where  $N_{\text{shift}} = 0$  is the conventional choice. We will instead consider the combination of choosing  $N_{\text{shift}} = 1$  for natural-parity states and  $N_{\text{shift}} = 0$  for unnatural-parity states. This choice implies that we will have the same  $H_{\text{eff}}$  for both positive- and negative-parity states in adjoining model spaces, e.g., the  $N_{\text{max,eff}} = 1$  effective Hamiltonian will be used in both

the  $N_{\max} = 0$  and  $N_{\max} = 1$  model spaces. The logic for the revised strategy stems from four considerations: (1) either strategy will converge to the exact result in sufficiently large model spaces; (2) the relative position of positive- and negative-parity states will converge faster when the same effective Hamiltonian is used for both of them; (3) for adjoining spaces in heavier systems, the predominant sets of pairwise interactions are in the same configurations with just one pair at a time shifting to the larger space; and (4) for electromagnetic transitions between states of opposite parity, the theory of the corresponding effective operators will be simplified. In addition to these four considerations, the revised strategy simplifies our work to compute  $H_{\text{eff}}$  since it is required only for every other increment in the basis space, such as  $N_{\max, \text{eff}} = 1, 3, 5, \dots$ , to evaluate the converging sequence.

In the next section we will explicitly illustrate the first two points by presenting results from large-scale calculations for two p-shell nuclear systems:  ${}^6\text{Li}$  and  ${}^9\text{Be}$ . The third point was highlighted in two recent papers applying the NCSM to systems with  $A = 47\text{--}49$  in restricted many-body model spaces [10, 11]. In those papers, the authors particularly argued that the bulk of the binding should not be altered in proceeding from a  $0\hbar\Omega$  to a  $1\hbar\Omega$  model space in  $A = 48$ , suggesting the same  $H_{\text{eff}}$  is preferred. Finally, the fourth consideration is useful for applications of the NCSM formalism involving transitions between states of different parities; and consequently for the future description of low-energy reactions such as electric dipole radiative capture processes.

## IV. RESULTS

### A. Converging sequences: different $N_{\text{shift}}$

We have performed calculations for  ${}^6\text{Li}$  up through the  $16\hbar\Omega$  ( $N_{\max} = 16$ ) model space, and for  ${}^9\text{Be}$  up through the  $10\hbar\Omega$  ( $N_{\max} = 10$ ) model space. The maximum dimensions of the encountered model spaces are  $d_p = 7.9 \times 10^8$  and  $d_p = 5.4 \times 10^8$  for  ${}^6\text{Li}$  and  ${}^9\text{Be}$ , respectively.

Most of the results presented in this paper are obtained using the nonlocal CD-Bonn 2000 (CDB2k) potential [19], which is a charge-dependent  $NN$  interaction based on one-boson exchange. The off-shell behavior of the CDB2k interaction differs from local potentials which leads to larger binding energies in nuclear few-body systems. Still, the CDB2k gives underbinding of nuclear many-body systems as is typical for standard high-precision  $NN$  interactions. In general, the CDB2k potential applied in the NCSM gives a good convergence rate and a weak HO frequency dependence.

A more recent realistic, nonlocal  $NN$  interaction, obtained through an inverse scattering analysis of the  $NN$  data, is able to provide reasonable binding energies of p-shell nuclei and is called the ‘‘JISP16’’ interaction [20]. We will use this interaction in Sec. IV B to illustrate the value of exponential fits to converging sequences in the NCSM.

The optimal HO frequency for each isotope was found by performing a series of calculations for a number of different frequencies and model spaces. We searched for the region in which the dependence on  $\hbar\Omega$  is minimal; and we selected this frequency (from the calculation in the largest model space) to

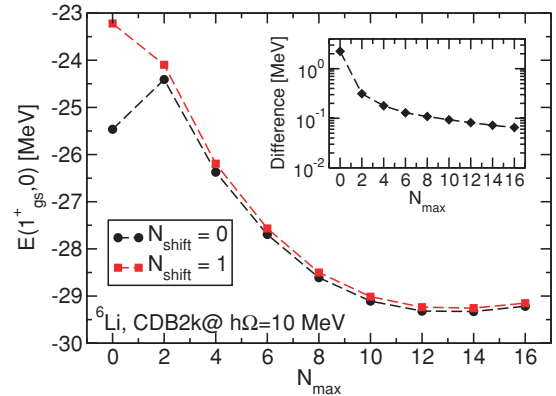


FIG. 1. (Color online) Ground-state binding energy of  ${}^6\text{Li}$  calculated with the CDB2k Hamiltonian with  $\hbar\Omega = 10$  MeV. Results obtained using two-body effective interactions generated with  $N_{\text{shift}} = 0$  and  $N_{\text{shift}} = 1$  are compared.

use in the more detailed investigation. In this way we found that the optimal frequencies for the CDB2k interaction are  $\hbar\Omega = 10$  MeV for  ${}^6\text{Li}$  and  $\hbar\Omega = 12$  MeV for  ${}^9\text{Be}$  (see also Ref. [21]). Since we will also use the  $N_{\max} + 1$  effective Hamiltonian for natural-parity states, diagonalized in the  $N_{\max}$  model space, we verified by explicit calculations that the same choices of optimal frequencies apply.

Note that the choice of optimal frequency is dependent on the model space used in the calculations. Consequently, a larger HO frequency ( $\hbar\Omega = 13$  MeV) was employed in an earlier NCSM study of  ${}^6\text{Li}$ , in which the calculations were limited to  $N_{\max} \leq 10$  [3].

The ground-state binding energy of  ${}^6\text{Li}$ , as a function of increasing model space  $N_{\max}$ , is presented in Fig. 1. The results obtained using the traditional cutoff for evaluating the effective interaction,  $N_{\max, \text{eff}} = N_{\max}$ , is represented by black circles, while the results obtained with  $N_{\max, \text{eff}} = N_{\max} + 1$  is represented by red squares. A number of observations can be made: First, these calculations demonstrate that the NCSM with the cluster-approximated effective interaction is not a variational approach. Convergence is not necessarily from above. Second, the difference between the two strategies for computing the effective interactions is the largest for small model spaces. The choice  $N_{\max, \text{eff}} = N_{\max} + 1$  reduces the excursions in the renormalized results in the lowest basis spaces as a function of  $N_{\max}$ . Third, both strategies converge to the same value as  $N_{\max} \rightarrow \infty$ . The binding-energy difference between the two calculations is plotted on a semilogarithmic scale in the inset of Fig. 1. We find that the convergence rate toward zero difference is exponential. The observed difference in our largest model space ( $N_{\max} = 16$ ) is less than 70 keV (corresponding to  $\sim 0.2\%$  of the total binding energy).

We present the results of a similar comparison for  ${}^9\text{Be}$  in Fig. 2. The spectroscopy and various properties of this nucleus were extensively studied within the NCSM approach in Ref. [21]. The same observations as for  ${}^6\text{Li}$  concerning the convergence rate apply for this case, although with  $A = 9$  we are slightly further from converged results. Still, we find an exponential convergence rate toward zero difference between the two strategies, as shown in the lower panel of Fig. 2.

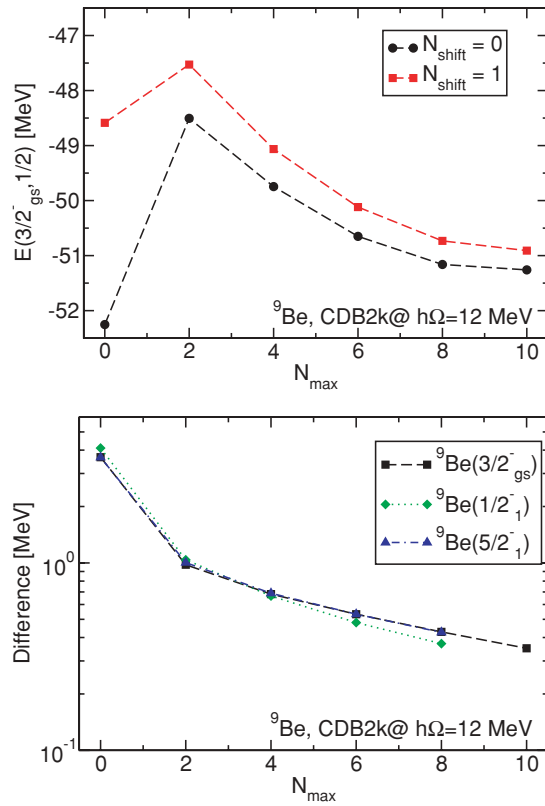


FIG. 2. (Color online) Upper panel: Ground-state binding energy of  ${}^9\text{Be}$  calculated with the CDB2k Hamiltonian with  $\hbar\Omega = 12$  MeV. Results obtained using two-body effective interactions generated with  $N_{\text{shift}} = 0$  and  $N_{\text{shift}} = 1$  are compared. Lower panel: Difference between binding energies computed with  $N_{\text{shift}} = 0$  and  $N_{\text{shift}} = 1$  for the first three natural-parity states of  ${}^9\text{Be}$ .

We studied three different, low-lying natural-parity states and found the same convergence pattern. For the ground state calculated in the  $N_{\text{max}} = 10$  model space, the difference in computed binding energy is 350 keV ( $\leq 0.7\%$  of the total binding energy).

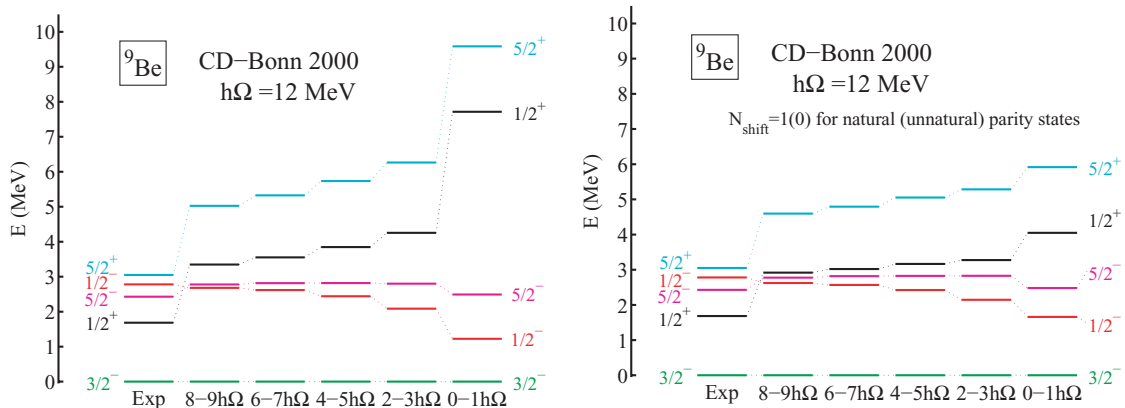


FIG. 3. (Color online) Spectrum of natural- and unnatural-parity states of  ${}^9\text{Be}$  calculated with the CDB2k Hamiltonian with  $\hbar\Omega = 12$  MeV. The natural-parity states are obtained using two-body effective interactions generated with  $N_{\text{shift}} = 0$  (left panel) or  $N_{\text{shift}} = 1$  (right panel).

As an additional remark, we note that the eigenenergies obtained with the  $N_{\text{max}} + 1$  effective interaction are always above the ones obtained with the  $N_{\text{max}}$  effective interaction. This observation persists for other systems that we have studied. An indication of the underlying reason for this observation can be obtained from the following argument: The  $N_{\text{max}} + 1$  effective interaction can be diagonalized in the  $N_{\text{max}} + 1$  model space, but we choose to diagonalize it in the  $N_{\text{max}}$  model space. Thus, we have a truncation of the “available” basis space so the result will be above the one with the same Hamiltonian in the full “available” space. This argument does not prove though, that it will always be above the results in the  $N_{\text{max}}$  basis space with the  $N_{\text{max}}$  effective Hamiltonian.

Up until now we have demonstrated that the two strategies converge to the same value, and that the  $N_{\text{max}} + 1$  effective interaction gives better renormalized results in the smallest ( $0\hbar\Omega$ ) model space. We also want to show that the relative position of positive- and negative-parity states converges faster when they are obtained by diagonalizing the same effective Hamiltonian. This claim is supported by the results presented in Fig. 3. In this figure, the combined spectrum of natural- and unnatural-parity states of  ${}^9\text{Be}$  is plotted. The two panels show the evolution of the spectra with increasing model spaces for the two strategies: (left) different effective Hamiltonians for each separate model space; and (right) the same effective Hamiltonian for each pair of model spaces,  $N_{\text{max}} = (0-1), (2-3), (4-5), \dots$ . The evaluated experimental spectrum [22] is shown in the leftmost column. Indeed, we find that the relative position of positive- and negative-parity states is better described already for small model spaces with the  $N_{\text{max}} + 1$  effective interaction being used for the natural-parity states.

Exponential fits to the calculated eigenenergies of the first natural- and unnatural-parity states are shown in Fig. 4. The two sequences of calculations of  $E(3/2^-_{g.s.})$  (with  $N_{\text{shift}} = 0$  and  $N_{\text{shift}} = 1$ , respectively) constitute an example of a series of converging sequences that converge to the same exact result. Therefore, we carry out a constrained fit of the two data sets. We use exponential functions and the constraint for

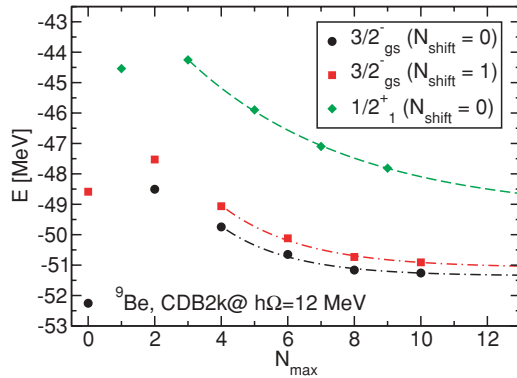


FIG. 4. (Color online) Basis size dependence of the calculated  $E(3/2_{gs}^-)$  and  $E(1/2_1^+)$  binding energies. The CDB2k Hamiltonian with  $\hbar\Omega = 12$  MeV is used. The binding energy of the (natural-parity) ground state is obtained using two-body effective interactions generated with  $N_{\text{shift}} = 0$  (black circles) and  $N_{\text{shift}} = 1$  (red squares). See text for details.

the fit is to have a common asymptote to both sequences. The fit produces a common asymptote of  $-51.40$  MeV with uncertainty of about 200 keV. In carrying out this constrained fit, the chi-square weights were based on the local derivative with respect to  $N_{\text{max}}$  so that results with minimal sensitivity to  $N_{\text{max}}$  receive greater weight. The  $N_{\text{max}} = 0-2$  results were excluded from the fit. We attempted alternative functional forms, such as  $\alpha + \beta N_{\text{max}}^{-\gamma}$ , but found none to be as successful as the constrained exponential fits shown in Fig. 4. Finally, we present in Fig. 5 a plot of the excitation energy of the first unnatural-parity state in  ${}^9\text{Be}$ , relative the natural-parity ground state, as a function of the model space size for the two different strategies. These results illustrate rather clearly that the relative position of natural- and positive-parity states is better described in the revised strategy where the same effective Hamiltonian is being used for diagonalization in both  $N_{\text{max}}$  and  $N_{\text{max}} + 1$  model spaces. The dashed lines correspond to the differences between the eigenenergy fits of Fig. 4. The

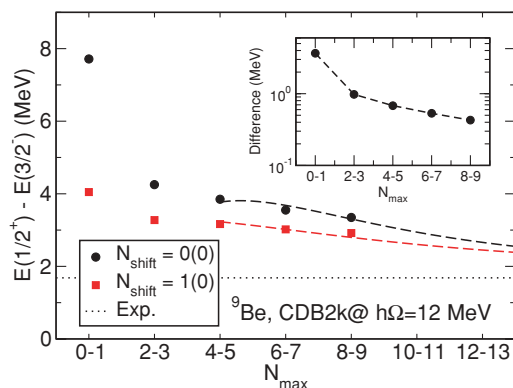


FIG. 5. (Color online) Basis size dependence of the calculated  $E_x(1/2_1^+)$  excitation energy relative to the lowest negative-parity state. The CDB2k Hamiltonian with  $\hbar\Omega = 12$  MeV is used. The binding energy of the (natural-parity) ground state is obtained using two-body effective interactions generated with  $N_{\text{shift}} = 0$  (black circles) and  $N_{\text{shift}} = 1$  (red squares).

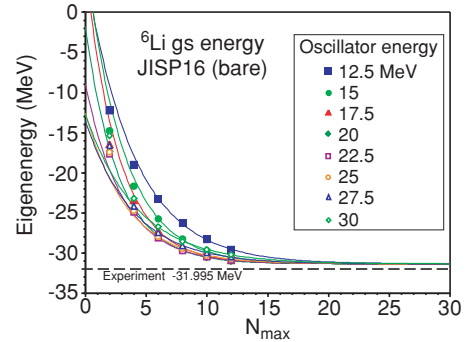


FIG. 6. (Color online) Ground-state binding energy of  ${}^6\text{Li}$  calculated with the JISP16 Hamiltonian for different HO frequencies ( $\hbar\Omega = 12.5-30$  MeV). The curves are extrapolated using a constrained exponential fit as described in the text.

common asymptote is  $E_x(1/2_1^+) = 2.10$  MeV. The difference in excitation energy between the two calculations is plotted on a semilogarithmic scale in the inset of Fig. 5.

### B. Converging sequences: different $\hbar\Omega$

Additional examples of series of converging sequences in the *ab initio* NCSM can be found. In the following we present a series of calculations of the ground state eigenvalue of  ${}^6\text{Li}$  using the JISP16 realistic  $NN$  interaction [20]. Figure 6 displays the results for the bare interaction as a function of  $N_{\text{max}}$  up through  $N_{\text{max}} = 12$ . In this case the series consists of the eight sequences of calculations for increasing model spaces performed at different HO frequencies, ranging from  $\hbar\Omega = 12.5-30$  MeV. The  $N_{\text{max}} = 0$  results are suppressed. These calculations should all converge to the same result as the dependence on the choice of HO frequency disappears with increasing model space. In addition, the procedure is variational due to the use of bare interactions. We carry out a constrained fit using exponential functions for each sequence at fixed  $\hbar\Omega$  using only the  $N_{\text{max}} = 6$  through  $N_{\text{max}} = 12$  results. The constraint for the fit is to have a common asymptote to all sequences. The uniformity of the convergence is striking and produces a common asymptote of  $-31.33$  MeV with uncertainty of about 100 keV. Again, the chi-square weights used in the fit were based on the local derivative with respect to  $N_{\text{max}}$  so that results with minimal sensitivity to  $N_{\text{max}}$  receive greater weight. We attempted alternative functional forms but found none to be as successful as the constrained exponential fits shown in Fig. 6.

## V. CONCLUSION

The *ab initio* NCSM is generally characterized by providing very fast convergence of many observables with increasing model space. This property is obviously very valuable when applying the method to studies of many-body nuclear systems. The existence of multiple converging sequences is another important property of the method; but one that has not been extensively utilized in the past. In this paper we have demonstrated the existence of multiple converging sequences

in the *ab initio* NCSM, and we have discussed some benefits of this property for certain applications. In particular, we have proposed a revised strategy for computing cluster-approximated effective interactions for  $A$ -body calculations in restricted model spaces.

The fundamental principle that motivated this work is a particular property of the theory of effective operators employed in the NCSM; namely that convergence to the exact results is guaranteed for any sequence that returns the bare Hamiltonian as the model space is increased,  $N_{\max} \rightarrow \infty$ . It was shown in Secs. III and IV that the specific choice of employing the same effective Hamiltonian for calculations in adjacent  $A$ -body model spaces resulted in some attractive convergence properties. Firstly, it was shown that it moderates the excursions in the renormalized results that are usually encountered when performing calculations in smaller model spaces, and secondly, that it gives a faster convergence of the relative position of binding energies of opposite parity states. We also demonstrated, by explicit large-scale calculations, that the revised strategy indeed converges to the same result as the traditional choice of using a  $N_{\text{shift}} = 0$  effective interaction for each model space. We suggested that this new strategy is particularly useful for studies of nuclear systems in which states of both parities are simultaneously involved. Use of the revised strategy is specifically envisioned for calculations of electromagnetic transitions between states of opposite parities, as the theory of the corresponding effective operator is simplified.

Another class of converging sequences was demonstrated by performing calculations using the bare JISP16 realistic  $NN$  interaction for a series of HO frequencies. In this case, our approach obeys the variational principle; for each choice of  $\hbar\Omega$  we are guaranteed to approach the exact result from above. In addition, all sequences are guaranteed to converge to the same result as  $N_{\max} \rightarrow \infty$ . We utilized this property by carrying out fits to all sequences using exponential functions, with the constraint to have a common asymptote. This approach is potentially very useful for gaining confidence in extrapolated results and for estimating their uncertainties.

### ACKNOWLEDGMENTS

This work was partly performed under the auspices of the US Department of Energy by the University of California, Lawrence Livermore National Laboratory under contract no. W-7405-Eng-48. One of us (C.F.) acknowledges financial support from Stiftelsen Lars Hiertas Minne and from Stiftelsen Långmanska Kulturfonden. One of us (J.V.) acknowledges support from the US Department of Energy Grant no. DE-FG02-87ER40371. The calculations reported here were partly performed on computational resources supplied by The Swedish National Infrastructure for Computing (SNIC) under project SNIC007-07-56.

- 
- [1] P. Navrátil, J. P. Vary, and B. R. Barrett, Phys. Rev. Lett. **84**(25), 5728 (2000).
  - [2] P. Navrátil, J. P. Vary, and B. R. Barrett, Phys. Rev. C **62**, 054311 (2000).
  - [3] P. Navrátil, J. P. Vary, W. E. Ormand, and B. R. Barrett, Phys. Rev. Lett. **87**, 172502 (2001).
  - [4] J. da Providencia and C. M. Shakin, Ann. Phys. (NY) **30**, 95 (1964).
  - [5] K. Suzuki and S. Y. Lee, Prog. Theor. Phys. **64**, 2091 (1980).
  - [6] K. Suzuki, Prog. Theor. Phys. **68**(1), 246 (1982).
  - [7] K. Suzuki and R. Okamoto, Prog. Theor. Phys. **70**, 439 (1983).
  - [8] K. Suzuki and R. Okamoto, Prog. Theor. Phys. **92**, 1045 (1994).
  - [9] C. P. Viazminsky and J. P. Vary, J. Math. Phys. **42**(5), 2055 (2001).
  - [10] J. P. Vary, S. Popescu, S. Stoica, and P. Navrátil, nucl-th/0607041.
  - [11] J. P. Vary, A. G. Negoita, and S. Stoica, nucl-th/0612022.
  - [12] D. C. J. Marsden, P. Navrátil, S. A. Coon, and B. R. Barrett, Phys. Rev. C **66**, 044007 (2002).
  - [13] P. Navrátil and W. E. Ormand, Phys. Rev. C **68**, 034305 (2003).
  - [14] S. C. Pieper, K. Varga, and R. B. Wiringa, Phys. Rev. C **66**, 044310 (2002).
  - [15] A. C. Hayes, P. Navrátil, and J. P. Vary, Phys. Rev. Lett. **91**, 012502 (2003).
  - [16] P. Navrátil, G. P. Kamuntavičius, and B. R. Barrett, Phys. Rev. C **61**, 044001 (2000).
  - [17] E. Caurier and F. Nowacki, Acta Phys. Pol. B **30**(3), 705 (1999).
  - [18] J. P. Vary, The Many-Fermion-Dynamics Shell-Model Code, Iowa State University, 1992 (unpublished); J. P. Vary and D. C. Zheng, *ibid.*, 1994 (unpublished).
  - [19] R. Machleidt, Phys. Rev. C **63**, 024001 (2001).
  - [20] A. M. Shirokov, J. P. Vary, A. I. Mazur, and T. A. Weber, Phys. Lett. **B644**, 33 (2007).
  - [21] C. Forssén, P. Navrátil, W. E. Ormand, and E. Caurier, Phys. Rev. C **71**, 044312 (2005).
  - [22] D. R. Tilley, J. H. Kelley, J. L. Godwin, D. J. Millener, J. E. Purcell, C. G. Sheu, and H. R. Weller, Nucl. Phys. **A745**, 155 (2004).